NUCLEAR ENGINEERING

MASSACHUSETTS INSTITUTE
OF TECHNOLOGY

MITNE-314

# GEOMETRICAL EFFECTS ON AXIAL &AZIMUTHAL VARIATIONS OF HEAT FLUX TO COOLANT IN ASYMMETRICALLY HEATED CHANNELS

**Chunyun Wang**
**Edited by Nina Lanza**

July 1998

MITNE-314

# GEOMETRICAL EFFECTS ON AXIAL &AZIMUTHAL VARIATIONS OF HEAT FLUX TO COOLANT IN ASYMMETRICALLY HEATED CHANNELS

**Chunyun Wang**
**Edited by Nina Lanza**

July 1998

## Abstract

This report summarizes analyses of the effects of heat conduction in a copper block on the heat flux to a coolant flowing axially in the block. Heat is assumed to be added through one side of the block corresponding to conditions that may arise in fusion reactors or particle accelerator targets. It is found that three dimensional analysis of the heat transport will be required to accurately describe the heat flux at the wall of the coolant channel. The effects of axial and azimuthal heat conduction in the copper block depend on the block width to channel diameter ratio and the BIOT number of the channel.

# Geometrical Effects on Axial & Azimuthal Variations of Heat Flux to Coolant in Asymmetrically Heated Channels

## 1. **Purpose**

There are only few empirical relations of heat transfer in a high-velocity flow (i.e. v = 10 ~20 m/s) of sub-cooled water with extremely high wall heat flux (i.e. q" $\geq$ 6 MW/m$^2$). In order to study this relationship, an experimental apparatus was built to investigate heat transfer under these conditions, and an analysis of the geometrical effects on the coolant heat flux has been made in order to guide the experimental design.

In the past, a copper block was uses for this experiment; however, this time an INCONEL 600 alloy tube was used as the test section. With the help of ADINA, the temperature distributions for two and three-dimensions were calculated for both the copper block and the INCONEL 600 tube at the given heat flux and heat.

ADINA is a finite element software developed by ADINA R&D Inc. which is installed on Athena of MIT; it can be run at an SGI workstation. The ADINA system includes the pre-processor ADINA-IN, the structural analysis program ADINA, the heat transfer program ADINA-T, the fluid flow program ADINA-F, and the post-processor ADINA-PLOT. The pre-processor ADINA-IN was used to define the geometry of the model, to discover the material properties and loads, and to create meshes, elements and nodes. Using the data file created by ADINA-IN as the input file of ADINA-T, the out files were obtained.

## 2. **2D and 3D ADINA models**

### 2.1 Models of the Copper Block

Fig.1 shows the schematic of the copper block: D denotes the channel diameter, H denotes height, W denotes width, and L denotes length. Because the copper block is symmetrical, only half the block was taken as the calculation model. The 2D ADINA model of the copper block is shown in Fig.2; looking at this figure, it is possible to see that the meshes close to the channel are denser than those in other places. An incident heat flux $q''_{in}$ was imposed at to the left side of the block, and heat convection was allowed between the top surface of the block and the air, as well as between the channel surface and coolant. In order to keep the node distribution agreement in each element, 9 nodes were created for each conduction element and 3 nodes were created for each convection element. Loads and boundary conditions are shown in Table 1.

The thermal conductivity of copper varies with temperature, and the values used in this experiment are shown in Table 2.

Table 1 Loads and Boundary Conditions in the 2D ADINA Model of the Copper Block

| | |
|---|---|
| Heat flux $q''_{in}$ | 6.5 MW/m$^2$ |
| Heat transfer coefficient at channel surface | 50,000 W/(m$^2$ °C) |
| Heat transfer coefficient at top surface | 5 W/(m$^2$ °C) |
| Bulk coolant temperature | 64 °C |
| Coolant pressure | 3 MPa |
| Air temperature | 20 °C |

Table 2 Values of Copper's Thermal Conductivity, as Used in the ADINA Model

| Temperature ( °C) | k (W/m °C) | Temperature ( °C) | k (W/m °C) |
|---|---|---|---|
| 0 | 401 | 527 | 371 |
| 27 | 398 | 627 | 364 |
| 77 | 394 | 727 | 357 |
| 127 | 392 | 827 | 350 |
| 227 | 388 | 927 | 342 |
| 327 | 383 | 1027 | 334 |
| 427 | 377 | 1085 | 329.36 |

The 3D ADINA model of the copper block is shown in Fig.3. In this model, the heat transfer coefficient of the channel surface and the bulk coolant temperature are varied axially. The other loads and boundary conditions are the same as those of the 2D model (see Table 1). The block was divided into 4 azimuthal sections of equal length; the heat transfer coefficient of the channel surface applying to each section, along the entire length from entrance to exit, are 100,000 W/(m$^2$ °C), 83,000 W/(m$^2$ °C), 67,000 W/(m$^2$ °C) and 50,000 W/(m$^2$ °C) respectively. The bulk coolant temperatures for each section are 23 °C, 36 °C, 50 °C and 64 °C respectively. Table 3 shows the loads and boundary conditions.

## 2.2 INCONEL 600 Tube Models

Figures 4 and 5 show the 2D ADINA models of asymmetrical and symmetrical INCONEL tubes. As Fig.4 shows, Ri is the channel radius, Ro1 is the outside surface radius, and Ro2 is the outermost surface radius. Unlike the copper block, there is no incident heat flux in the INCONEL models, but an internal heat generation is applied. The heat transfer coefficient at the channel surface as well as the bulk coolant temperature in

the channel are given as boundary conditions. The thermal conductivity of INCONEL is also varied with the temperature as shown in Table 4.

Table 3 Loads and Boundary Conditions in 3D ADINA Model of Copper Block

| | Section I (Entrance) | Section II | Section III | Section IV (Exit) |
|---|---|---|---|---|
| Heat flux $q''_{in}$ (MW/m$^2$) | 6.5 | 6.5 | 6.5 | 6.5 |
| Heat transfer coefficient at channel surface (W/m$^2$ °C) | 100,000 | 83,000 | 67,000 | 50,000 |
| Heat transfer coefficient at top surface (W/m$^2$ °C) | 5 | 5 | 5 | 5 |
| Bulk coolant temperature (°C) | 23 | 36 | 50 | 64 |
| Coolant pressure (MPa) | 3.0 | 3.0 | 3.0 | 3.0 |
| Air temperature (°C) | 20 | 20 | 20 | 20 |

Table 4 INCONEL Thermal Conductivity Used in the ADINA Model

| Temperature ( °C) | k (W/m °C) | Temperature ( °C) | k (W/m °C) |
|---|---|---|---|
| -150 | 12.5 | 400 | 20.5 |
| -100 | 13.1 | 500 | 22.1 |
| -50 | 13.6 | 600 | 23.9 |
| 20 | 14.9 | 700 | 25.7 |
| 100 | 15.9 | 800 | 27.5 |
| 200 | 17.3 | 900 | 29.3 |
| 300 | 19.0 | 1000 | 31.1 |

## 3. **Results**

### 3.1 Flux Peaking Factor of the 2D Copper Block

For the copper block, the peaking factor is defined as PF = $\frac{q''_{ch}}{q''_{in}}$, the ratio of heat flux at the channel surface as $q''_{ch}$, and the incident heat flux as $q''_{in}$. The azimuthal angle θ is shown in Fig. 2. Fig. 6 depicts the dependence of the peaking factor on the azimuthal angle θ for three cases in which the channel radii are varied; both the height and width of the copper block are two times the diameter of its channel. If the peaking factor is defined as PF2= $\frac{q''_{ch}}{q''_{ch,av}}$, then $q''_{ch,av}$ is the average heat flux at the channel surface.

Fig. 7 shows the PF2 versus the azimuthal angle θ for three cases with different channel radii. In Figures 6 and 7, one should note that the azimuthal variation increases as the radius of the channel increases; because the geometrical properties, loads, and boundary conditions are proportional in the three cases, the average heat flux at the channel surface happens at the same azimuthal angle. Fig. 8 shows the azimuthal temperature distribution at the channel surface; note that the highest temperature (204.3 °C) at the channel surface is much lower than the saturation temperature (233.84 °C) in these three cases.

The Peaking Factor PF and Peaking Factor PF2 versus the azimuthal angle θ are shown in Figure 9 and 10; these are for the copper block with a height of 19mm, a width of 18.6mm, and a channel with a radius of 1.5 mm. The temperature at the channel surface is shown in Fig. 11; note that the azimuthal variation is within ± 9%. When the block has a height and width of 6mm each and a radius of 1.5mm, the azimuthal variation is a factor of two for both the peak and the minimum heat flux, and the temperature of any point on the channel surface is at least 73 °C higher than the saturation temperature.

### 3.2 Effect of the Biot Number on the 2D Copper Block

Figures 12 and 13 show the Peaking Factor (PF2) and the temperature distribution versus azimuthal angle for the following three cases: (1) Bi=150/k, Ri=4.5mm, W=18mm, H=18mm; (2) Bi=150/k, Ri=3mm, W=12mm, H=12mm; (3) Bi=225/k, Ri=4.5mm, H=18mm, W=18mm. Because the temperature on the channel surface did not vary much (less than 64.1 °C), the copper's thermal conductivity can be considered to be the same as at the channel surface in these three cases. Another consideration is that the Biot number is same in the first case as in the second case; from Fig.12, one can see that the Peaking Factor (PF2) curves coincide with the same Biot numbers. With the higher Bi number (250/k), the azimuthal variation is larger. From Fig.13, one can see that the temperature at the channel surface increases with an increasing channel radius, while at the same time keeping the same Bi number.

### 3.3 Effect of Three-Dimensional Heat Conduction of the Copper Block

Because the heat transfer coefficient at the channel surface and the bulk coolant temperature at the channel are varied axially, heat conduction exists axially in the copper block. In the 3D model, the heat transfer coefficient is 100,000 W/m$^2$ °C and the bulk temperature is 23 °C in the entrance section. They change from these values to 50,000 W/m$^2$ °C, and 64 °C respectively in the exit section.

Figures 14, 16, and 18 compare the 2D and 3D copper blocks' Peaking Factor (PF) for three cases: with channel radii of 1.5mm, 3 mm, and 4.5mm respectively. Figures 15, 17, and 19 are the temperature distribution azimuthally. In the three cases, the curves for the 3D block show the heat transfer situation in the exit section; one can see that the heat

transfer shape in the 3D exit section is same as that of the 2D model. However, the 3D model's Peaking Factor is less than the 2D's and the temperature is also less than the 2D model's at the same azimuthal angle; this indicates that a part of heat is transferred axially upstream through the copper block.

Figures 20 and 21 compare the different lengths of the 3D copper blocks. One can see that the longer copper block, the less heat will be transferred axially from the exit section to the entrance section.

## 3.4 The 2D INCONEL Tube

### 3.4.1 The 2D Symmetrical INCONEL Tube

Three cases were calculated for the fully symmetrical INCONEL tube. Table 5 shows the geometric properties, loads, and boundary conditions. Table 6 shows the calculation results: the temperature at the channel surface is much higher than the saturation temperature in all three cases.

Table 5 Properties of the 2D Symmetrical INCONEL Models

| | Case I | Case II | Case III |
|---|---|---|---|
| Inside surface radius Ri (mm) | 1.5 | 3.0 | 4.75 |
| Outside surface radius Ro (mm) | 2.0 | 3.5 | 5.13 |
| Internal heat generation q''' ($W/m^3$) | $2.914 \times 10^{10}$ | $3.138 \times 10^{10}$ | $4.289 \times 10^{10}$ |
| Heat transfer coefficient at channel surface ($W/(m^2\ °C)$) | 50,000 | 50,000 | 50,000 |
| Bulk coolant temperature (°C) | 59 | 59 | 59 |
| Coolant pressure (MPa) | 3.0 | 3.0 | 3.0 |

Table 6 Results of the 2D Symmetrical INCONEL Models Calculations

| | Case I | Case II | Case III |
|---|---|---|---|
| Temperature at inner surface (°C) | 398.967 | 398.950 | 398.929 |
| Temperature difference between inner and outside surface $\Delta T$ (°C) | 183.087 | 187.992 | 147.693 |
| Heat flux at the inner surface ($W/m^2$) | $1.7 \times 10^7$ | $1.7 \times 10^7$ | $1.7 \times 10^7$ |

3.4.2 The 2D Asymmetrical INCONEL Tube

Three cases were calculated for the asymmetrical INCONEL tube. Table 7 shows their geometric properties and loads. For INCONEL tube, the Peaking Factor is defined as PF2 $= \frac{q''_{ch}}{q''_{ch,av}}$, which is the same as the PF2 for copper block. Fig. 22 depicts the azimuthal distribution of the Peaking Factor (PF2); one can see that as the inner radius increases, the azimuthal variation increases for the peak heat flux, and the curve becomes steeper at the angles of 30° ~ 60°. This shows that the heat transferring from the thick cylindrical part to the thin cylindrical part will decrease as the inner surface's radius increases. Fig. 23 shows the temperature distribution azimuthally around the channel surface; note that the temperature of the channel surface in the thick cylindrical part of the INCONEL tube is higher than the saturation temperature by about 100 °C.

Table 7 Properties of the 2D Asymmetrical INCONEL Models

| | Case I | Case II | Case III |
|---|---|---|---|
| Inner surface radius Ri (mm) | 1.5 | 3.0 | 4.75 |
| Outside surface radius Ro1 (mm) | 2.0 | 3.5 | 5.13 |
| Most outside surface radius Ro2 (mm) | 2.74 | 4.33 | 6.13 |
| Internal heat generation q''' ($W/m^3$) | $2.914 \times 10^{10}$ | $3.138 \times 10^{10}$ | $4.289 \times 10^{10}$ |
| Coolant temperature (°C) | 74 | 59 | 59 |
| Coolant pressure (Mpa) | 3.0 | 3.0 | 3.0 |

3.5 Effect of Three-Dimensional Heat Conduction in the INCONEL Tube

For a 3D asymmetrical INCONEL tube with the inner surface radius of 1.5mm, an outside surface radius of 2.0mm, an outermost surface radius of 2.74mm, and a length of 50mm, the heat transfer coefficient at the channel surface and bulk coolant

Table 8 Loads and Boundary Conditions in 3D ADINA Model of INCONEL Tube

| | Section I (Entrance) | Section II | Section III | Section IV (Exit) |
|---|---|---|---|---|
| Internal heat generation q''' ($MW/m^3$) | $9.714x10^9$ | $9.714x10^9$ | $9.714x10^9$ | $9.714x10^9$ |
| Heat transfer coefficient at channel surface ($W/m^2$ °C) | 100,000 | 83,000 | 67,000 | 50,000 |
| Bulk coolant Temperature (°C) | 23 | 40 | 57 | 74 |
| Coolant pressure (MPa) | 3.0 | 3.0 | 3.0 | 3.0 |

temperature vary axially. The heat transfer coefficient is decreasing from the entrance section to the exit section: 100,000 W/($m^2$ °C), 83,000 W/($m^2$ °C), 67,000 W/($m^2$ °C) and 50,000 W/($m^2$ °C) respectively. The bulk coolant temperature is increasing axially: 23 °C, 40 °C, 57 °C and 74 °C respectively. Loads and boundary conditions in the 3D asymmetrical INCONEL tube are shown in Table 8; this is the ADINA model.

Figures 24 and 25 show the comparison of the 2D and 3D models' Peaking Factors (PF2), as well as the azimuthal temperature distribution of the asymmetrical INCONEL tube. The curves for the 3D model are the values in the exit section. The shape of the curves for the 3D block nearly coincide with that of the 2D model; in fact, the temperature difference at any point between the 2D and 3D models on the channel surface with the same azimuthal angle is less than 2 °C. The reason for these results can be explained by the fact that the conducting ability of the INCONEL tube is much lower than that of the copper blocks.

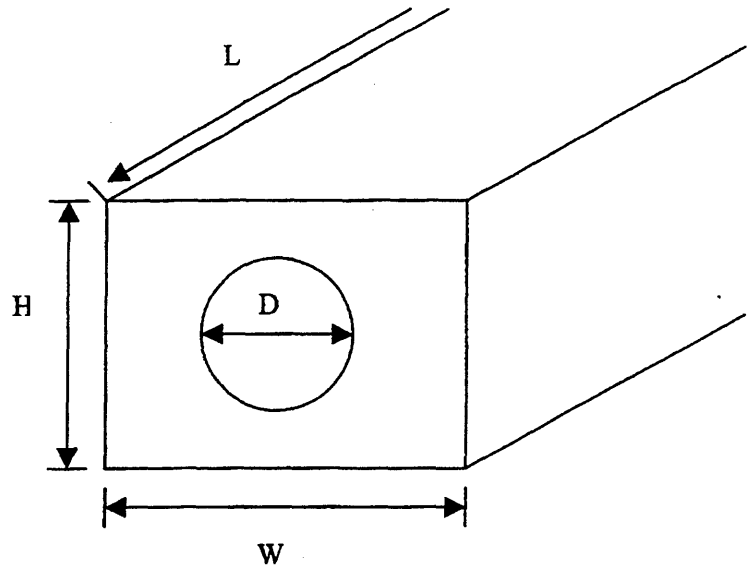


Fig.1 Schematic of the Copper Block

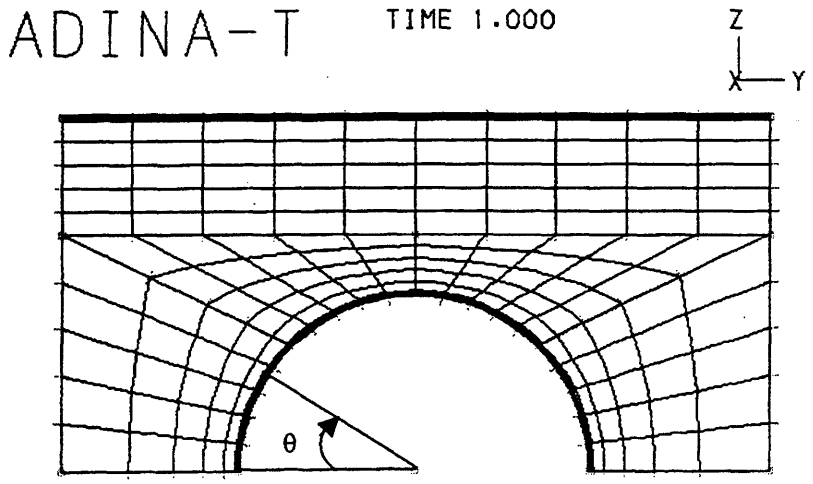


Fig. 2 2D ADINA Model for Copper Block

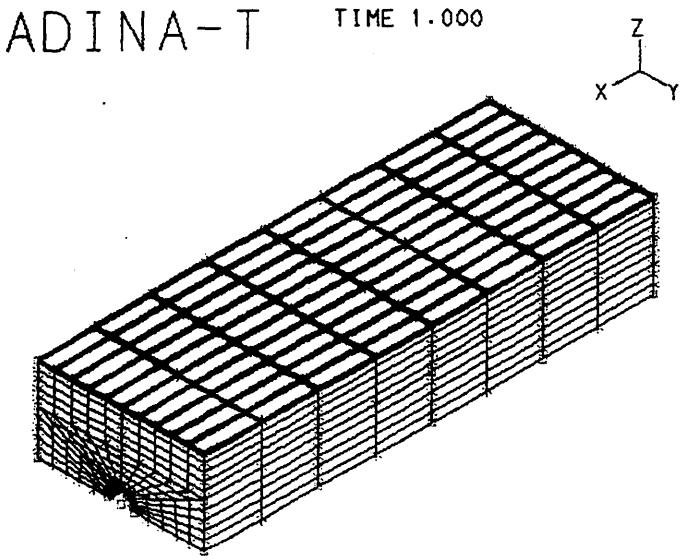


Fig. 3 3D ADINA Model for Copper Block

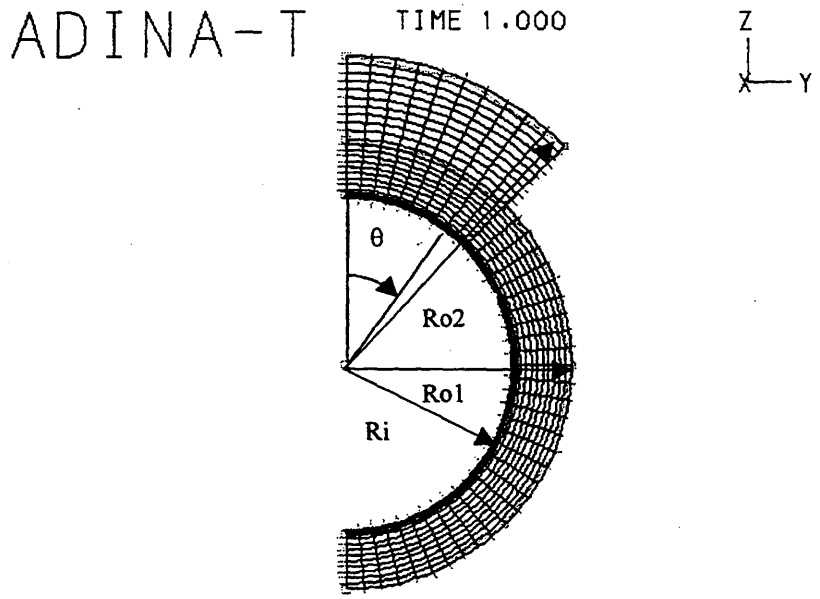


Fig. 4 2D ADINA Model for Asymmetrical INCONEL Tube

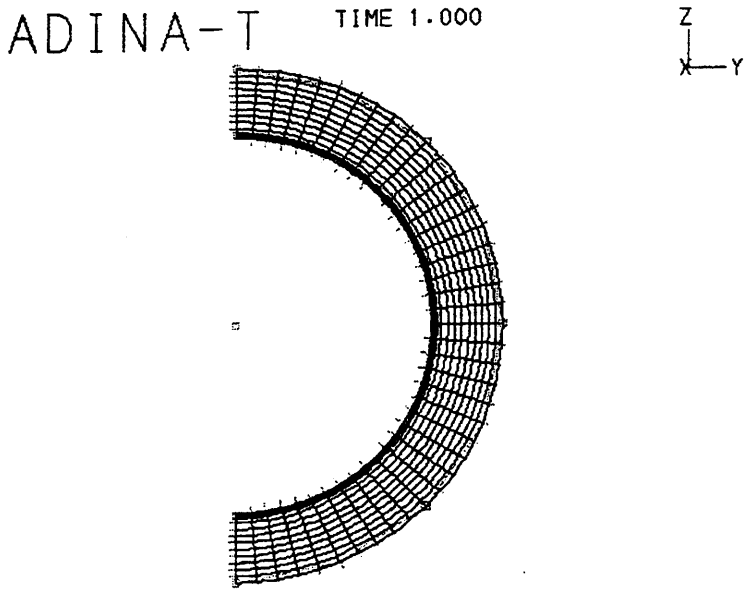


Fig. 5 2D ADINA Model for Symmetrical INCONEL Tube

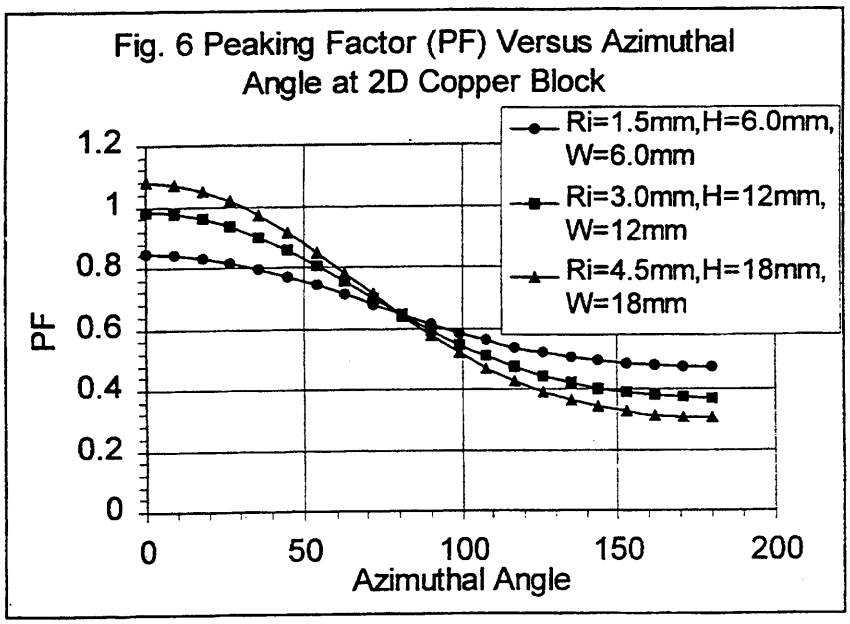

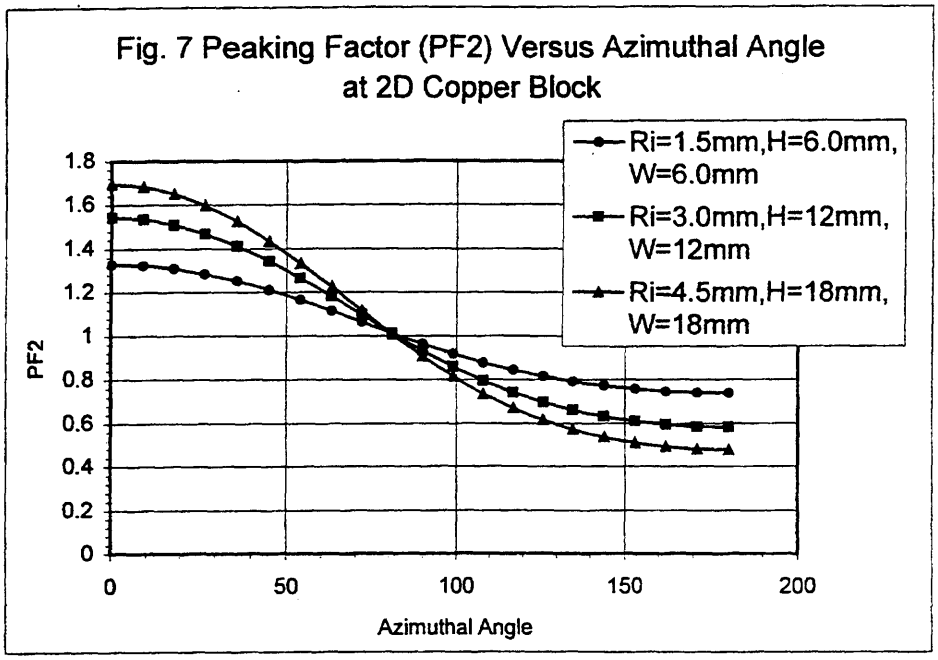
Fig. 7 Peaking Factor (PF2) Versus Azimuthal Angle at 2D Copper Block
Ri=1.5mm,H=6.0mm, W=6.0mm
Ri=3.0mm,H=12mm, W=12mm
Ri=4.5mm,H=18mm, W=18mm
PF2
1.8
1.6
1.4
1.2
1
0.8
0.6
0.4
0.2
0
0
50
100
150
200
Azimuthal Angle

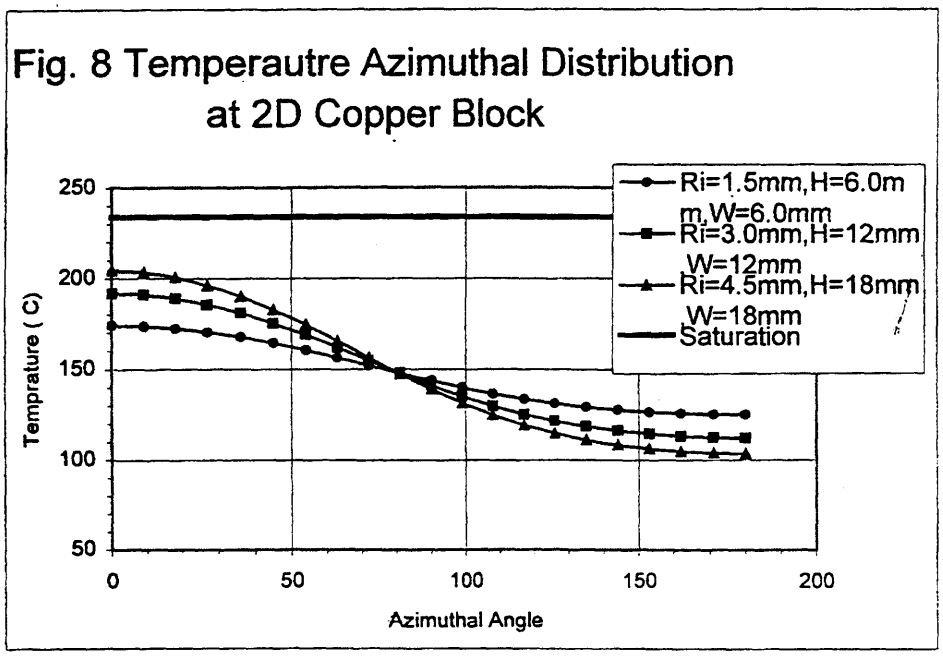
Fig. 8 Temperautre Azimuthal Distribution at 2D Copper Block
Ri=1.5mm,H=6.0mm,W=6.0mm
Ri=3.0mm,H=12mm W=12mm
Ri=4.5mm,H=18mm W=18mm
Saturation
Temprature ( C)
250
200
150
100
50
0
50
100
150
200
Azimuthal Angle

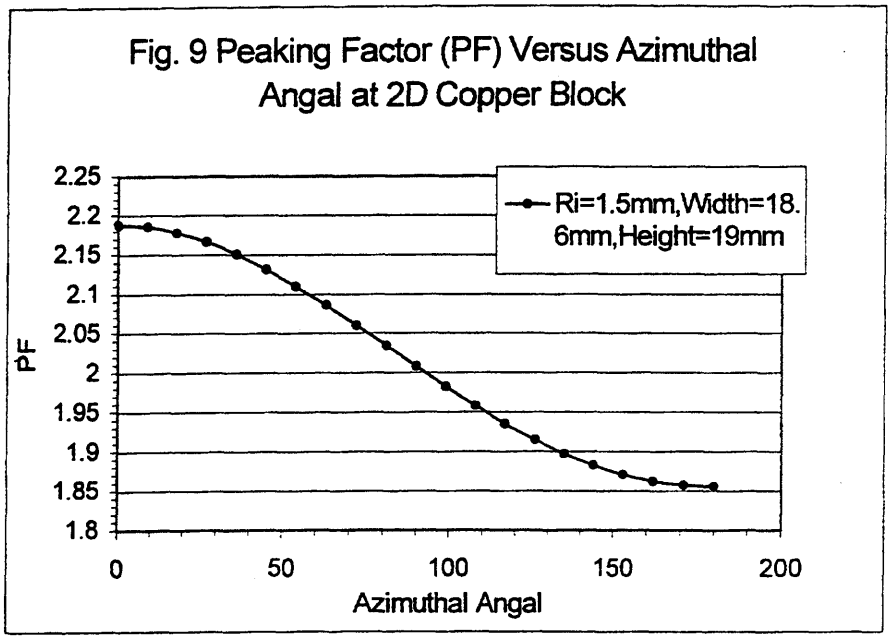
Fig. 9 Peaking Factor (PF) Versus Azimuthal Angal at 2D Copper Block
Ri=1.5mm,Width=18.6mm,Height=19mm
PF
2.25
2.2
2.15
2.1
2.05
2
1.95
1.9
1.85
1.8
0
50
100
150
200
Azimuthal Angal

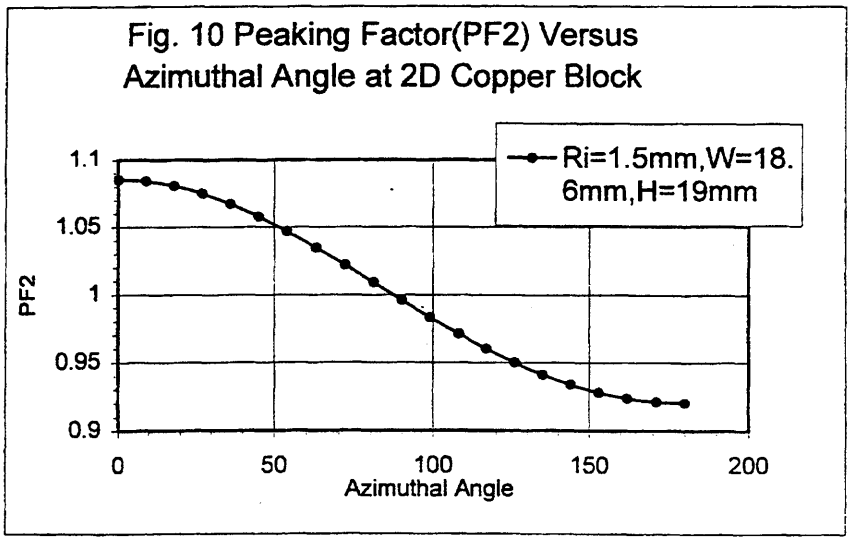
Fig. 10 Peaking Factor(PF2) Versus Azimuthal Angle at 2D Copper Block
Ri=1.5mm,W=18.6mm,H=19mm
PF2
1.1
1.05
1
0.95
0.9
0
50
100
150
200
Azimuthal Angle

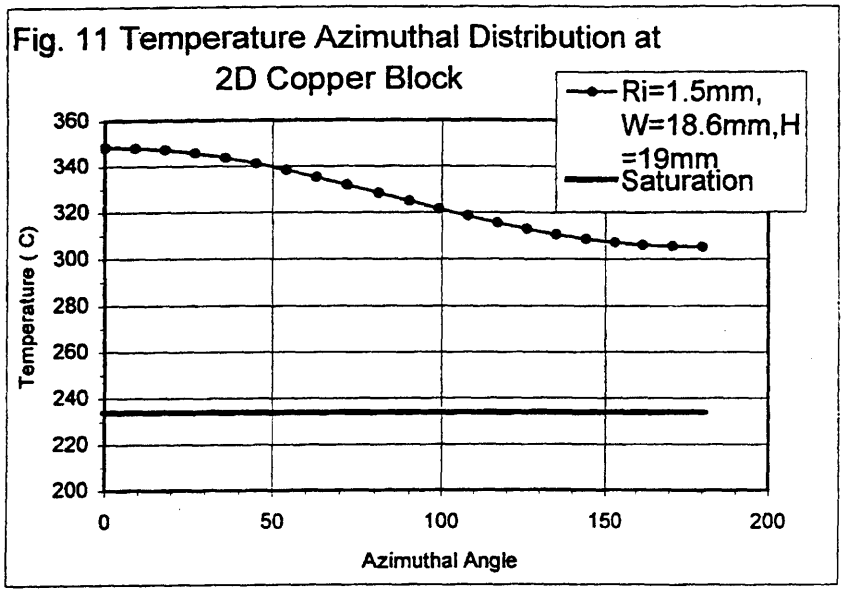
Fig. 11 Temperature Azimuthal Distribution at 2D Copper Block
Ri=1.5mm, W=18.6mm,H =19mm
Saturation
Temperature ( C)
360
340
320
300
280
260
240
220
200
0
50
100
150
200
Azimuthal Angle

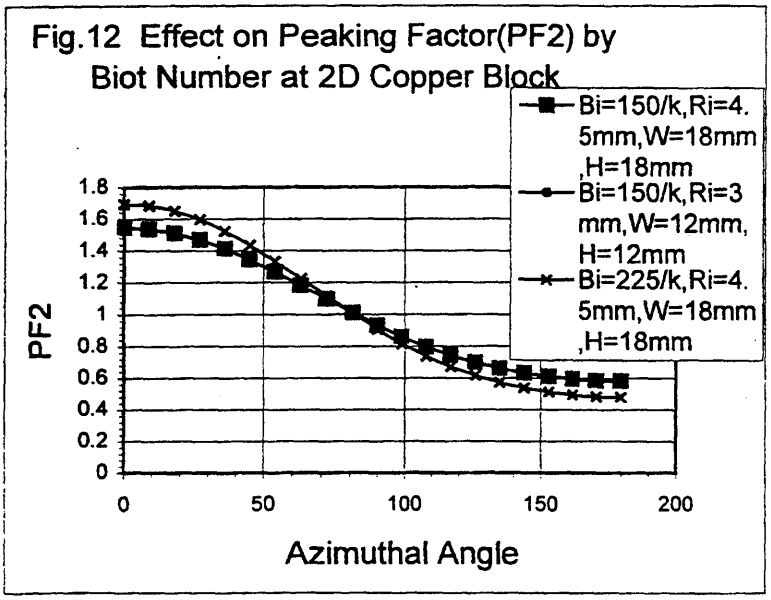
Fig.12 Effect on Peaking Factor(PF2) by Biot Number at 2D Copper Block
Bi=150/k,Ri=4.5mm,W=18mm ,H=18mm
Bi=150/k,Ri=3 mm,W=12mm, H=12mm
Bi=225/k,Ri=4.5mm,W=18mm ,H=18mm
PF2
1.8
1.6
1.4
1.2
1
0.8
0.6
0.4
0.2
0
0
50
100
150
200
Azimuthal Angle

Fig. 13 Effect on Temperature by Biot Number at 2D Copper Block

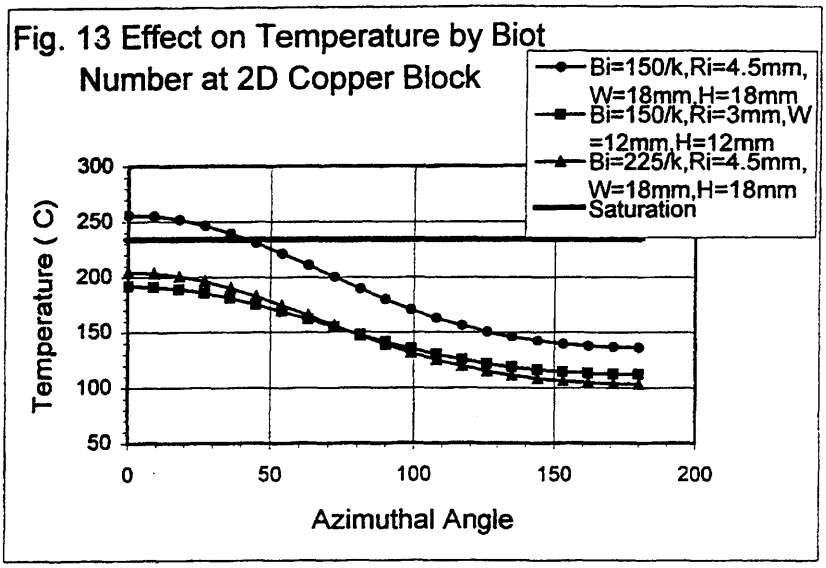


Fig. 14 Comparison 2D and 3D's Peaking Factor (PF) at Copper Block with Channel Radius 1.5mm

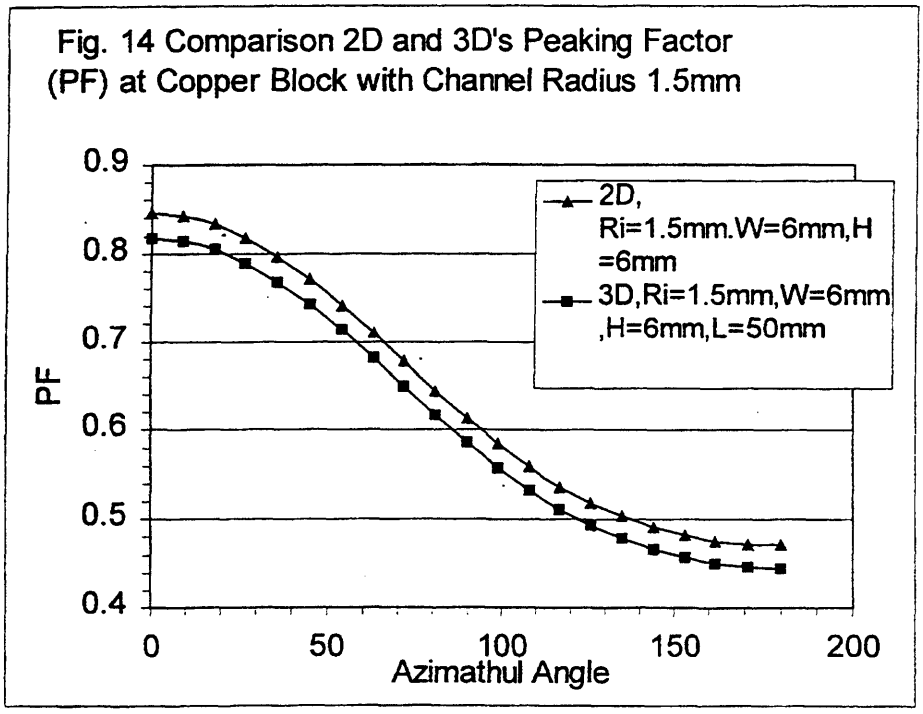

Fig. 15 Comparion 2D and 3D's Temperature Distribution at Copper Block with Radius 1.5mm

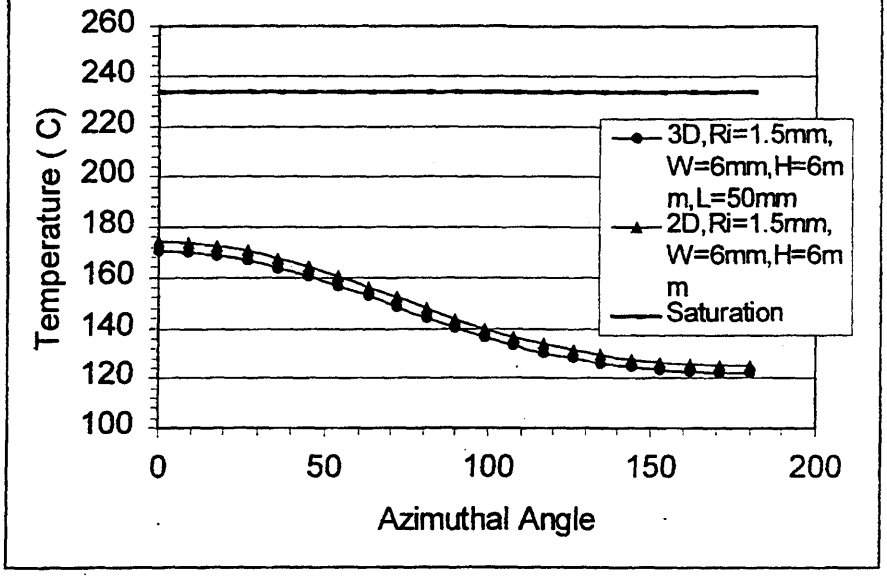


Fig. 16 Comparion 2D and 3D's Peaking Factor (PF) at Copper Block with Channel Radius 3mm

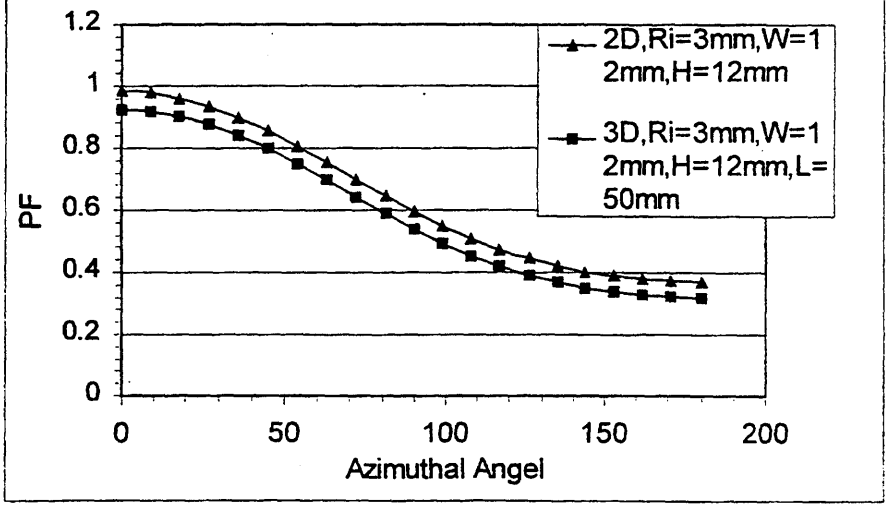

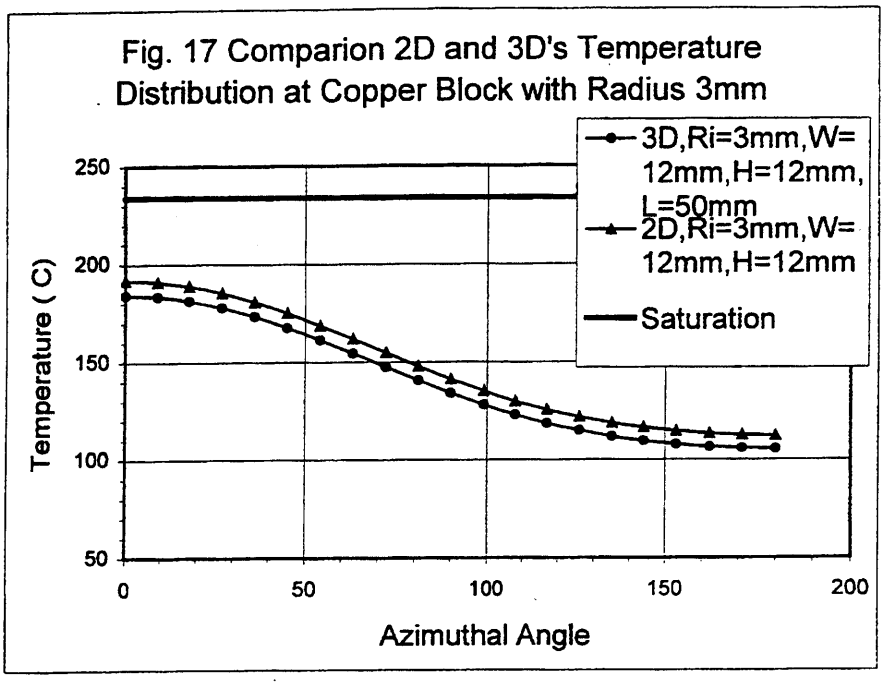
Fig. 17 Comparion 2D and 3D's Temperature Distribution at Copper Block with Radius 3mm
3D,Ri=3mm,W=12mm,H=12mm,L=50mm
2D,Ri=3mm,W=12mm,H=12mm
Saturation
Temperature ( C)
250
200
150
100
50
0
50
100
150
200
Azimuthal Angle

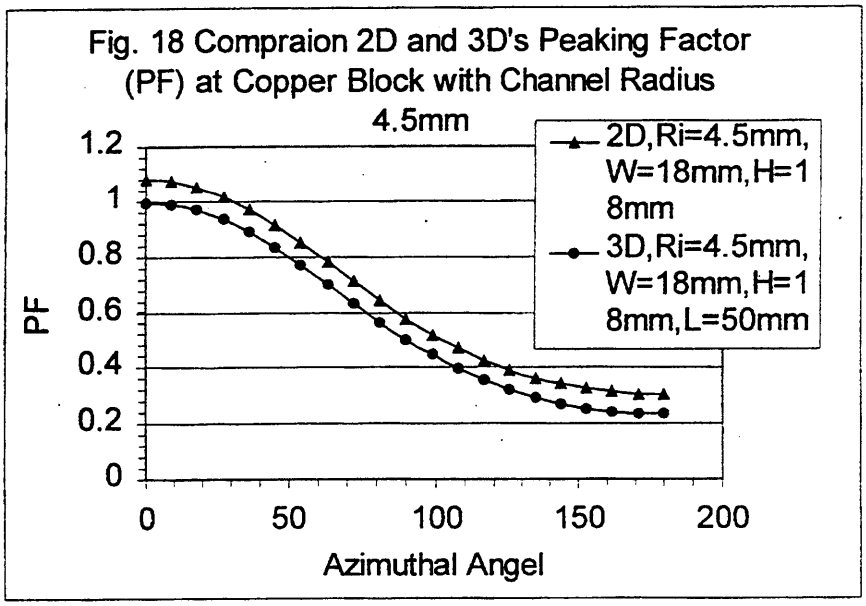
Fig. 18 Compraion 2D and 3D's Peaking Factor (PF) at Copper Block with Channel Radius 4.5mm
2D,Ri=4.5mm,W=18mm,H=18mm
3D,Ri=4.5mm,W=18mm,H=18mm,L=50mm
PF
1.2
1
0.8
0.6
0.4
0.2
0
0
50
100
150
200
Azimuthal Angel

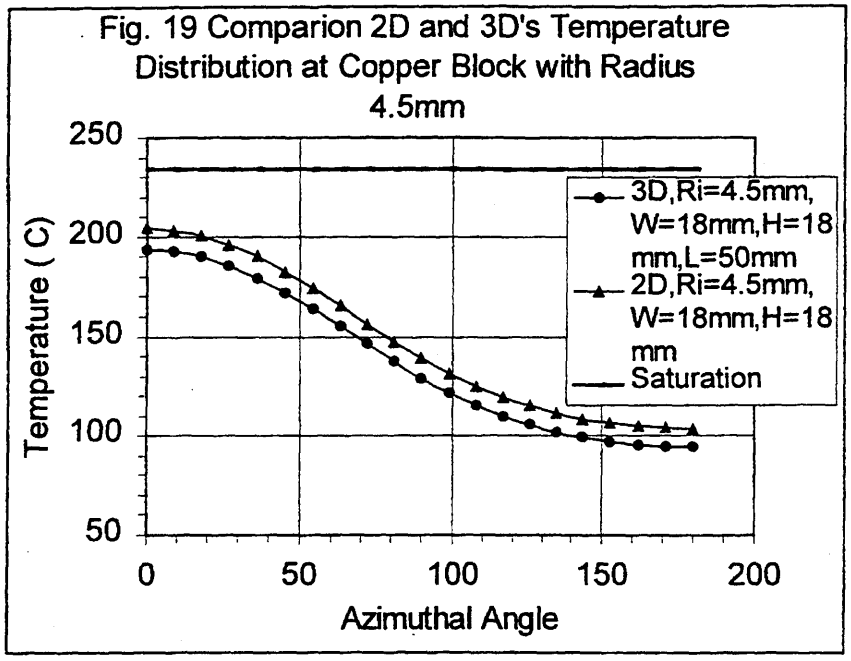
Fig. 19 Comparion 2D and 3D's Temperature Distribution at Copper Block with Radius 4.5mm
250
200
150
100
50
Temperature ( C)
0
50
100
150
200
Azimuthal Angle
3D,Ri=4.5mm, W=18mm,H=18 mm,L=50mm
2D,Ri=4.5mm, W=18mm,H=18 mm
Saturation

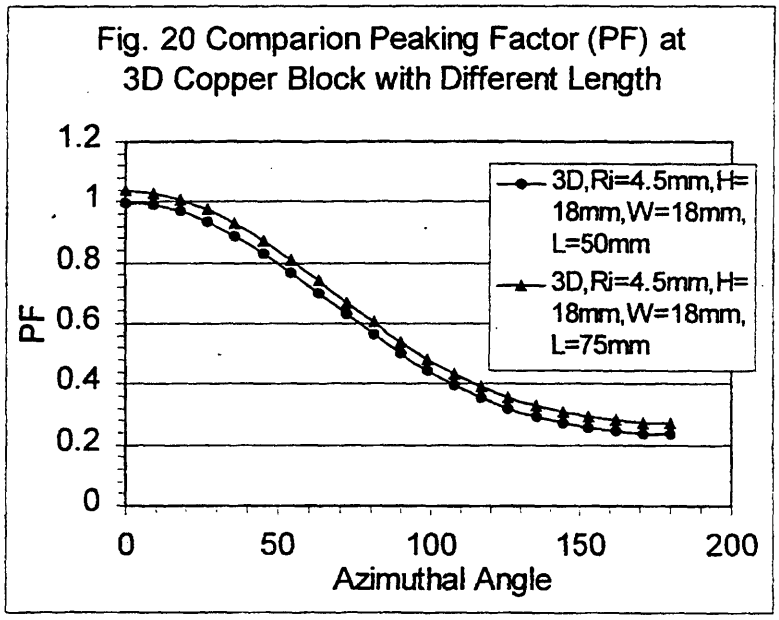
Fig. 20 Comparion Peaking Factor (PF) at 3D Copper Block with Different Length
1.2
1
0.8
0.6
0.4
0.2
0
PF
0
50
100
150
200
Azimuthal Angle
3D,Ri=4.5mm,H= 18mm,W=18mm, L=50mm
3D,Ri=4.5mm,H= 18mm,W=18mm, L=75mm

Fig. 21 Comparion Temperature Distribution at 3D Copper Block with Different Length

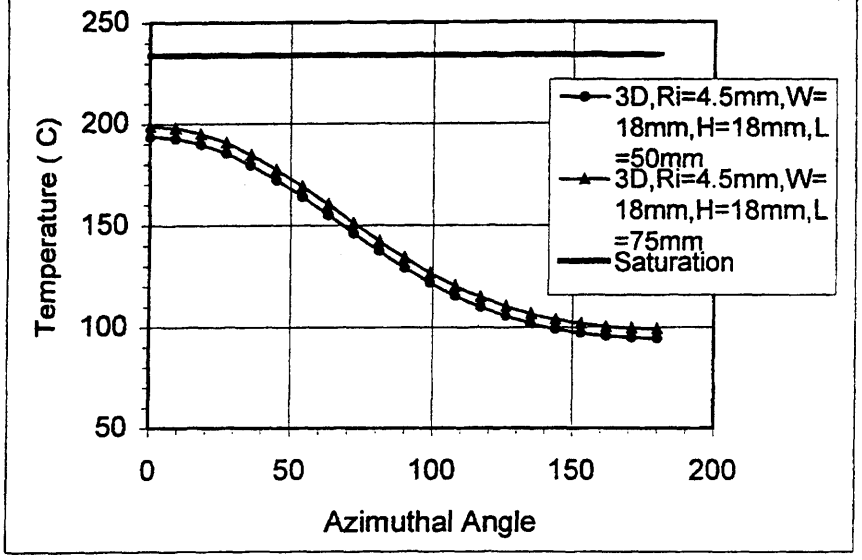


Fig. 22 Peaking Factor(PF2) Versus Azimuthal Angal at 2D Asymmetrical INCONEL Tube

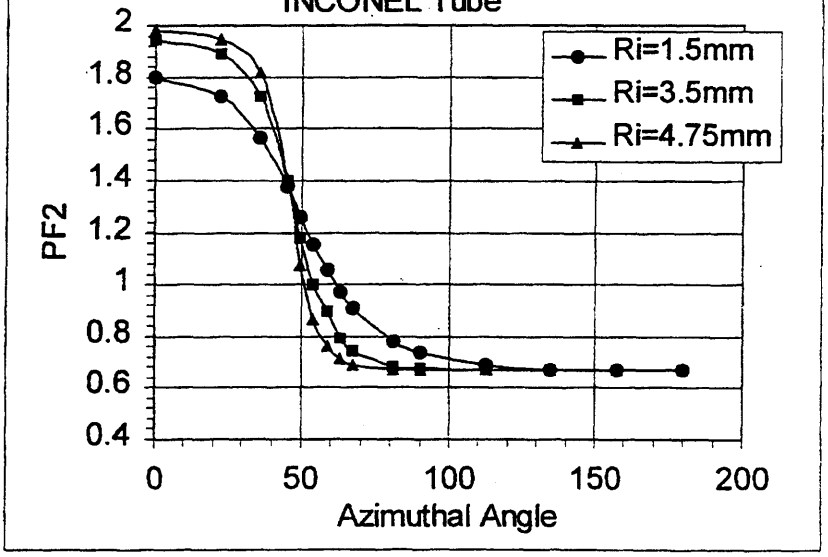

Fig. 23 Temperature Azimuthal Distribution at 2D Asymmetrical INCONEL Tube

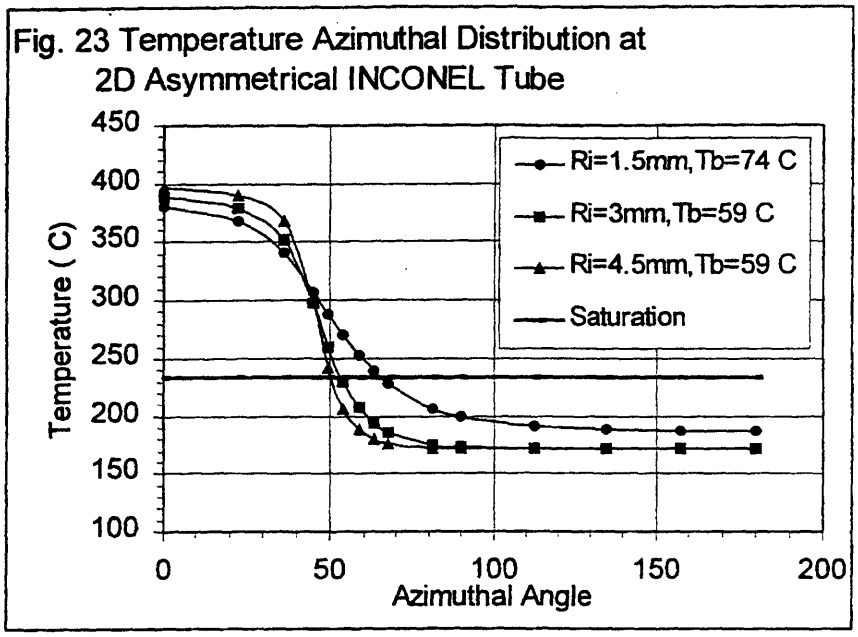


Fig. 24 Comparion 2D and 3D INCONEL Tube Peaking Factor (PF2) at Asymmetrical Cases with Ri=1.5mm,Ro1=2.0mm,Ro2=2.74mm,Tb=74 C

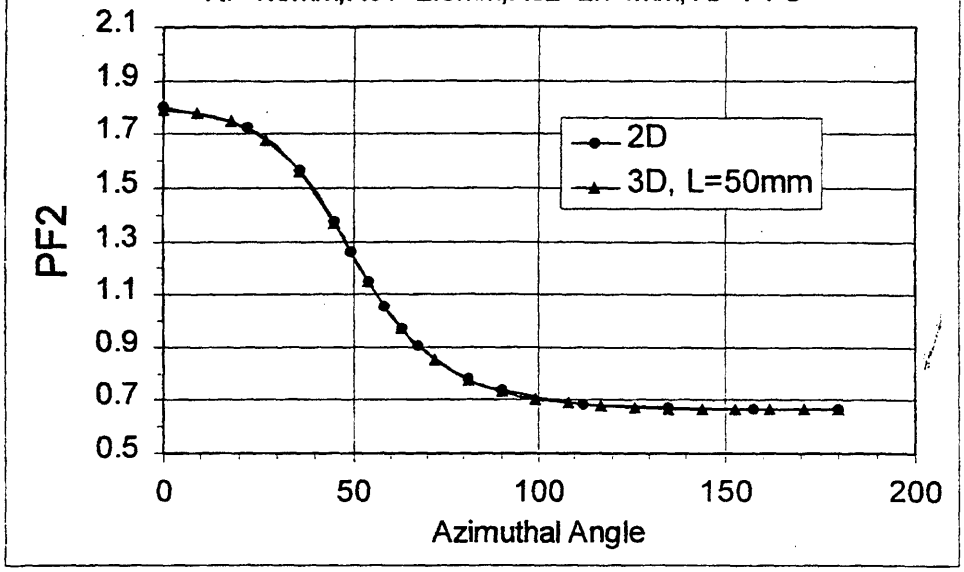

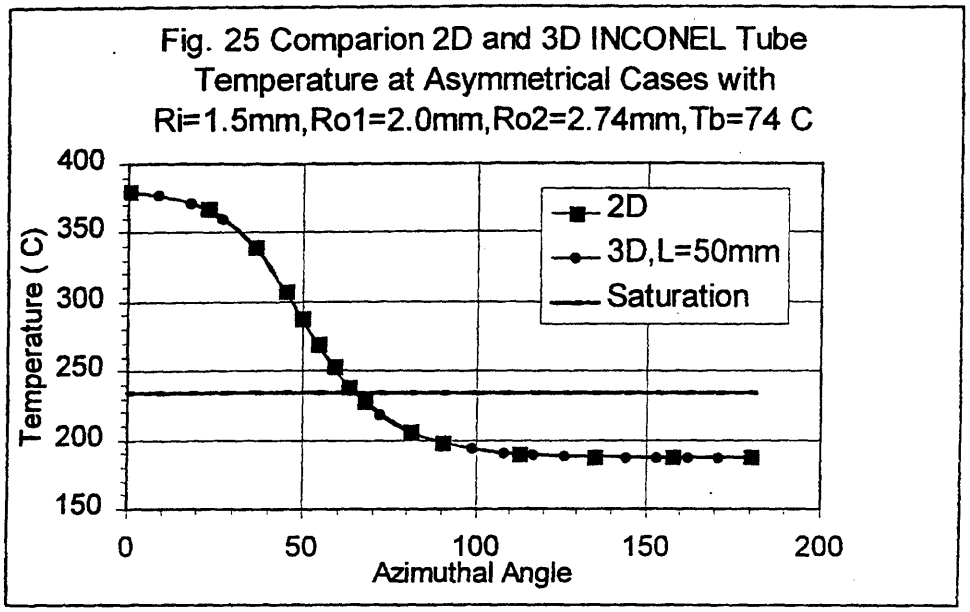
Fig. 25 Comparion 2D and 3D INCONEL Tube
Temperature at Asymmetrical Cases with
Ri=1.5mm,Ro1=2.0mm,Ro2=2.74mm,Tb=74 C
Temperature ( C)
400
350
300
250
200
150
0
50
100
150
200
Azimuthal Angle
2D
3D,L=50mm
Saturation